

## APPLICABILITY OF ENERGY-DISPERSIVE X-RAY POWDER DIFFRACTOMETRY TO DETERMINATIVE MINERALOGY

RAY E. FERRELL, JR., *Department of Geology, Louisiana State University, Baton Rouge, Louisiana 70803.*

### ABSTRACT

Powdered samples of quartz, calcite, kaolinite, chlorite, and muscovite were used to evaluate a new, rapid method of X-ray diffractometry. The technique employs a silicon semiconductor detector at a fixed diffraction angle and a multichannel analyzer to observe the wavelengths of a polychromatic X-ray beam diffracted by the sample.

The analysis of single mineral powders can be accomplished in 100 seconds, with recognizable patterns in as short a time as 10 seconds. The interpretation of spectra from multi-component samples is made difficult by the overlap of adjacent diffraction maxima.

### INTRODUCTION

X-ray powder diffraction methods are widely used in determinative mineralogy. Photographic or direct reading techniques are employed most frequently to identify unknown minerals in rocks and estimate quantitatively their abundance. Other uses of the powder diffraction method include crystal structure determinations, measurement of cell parameters, determination of the orientation of minerals in rocks, observation of temperature and pressure dependent phase changes, and the variation in the chemical composition in a solid solution series.

X-ray powder diffraction effects can be described simply in terms of the Bragg reflection analogy. Diffraction conditions are satisfied when:

$$\sin \theta = \lambda/2d(hkl)$$

where  $\theta$  is the angle of incidence between the primary X-ray beam and an atomic plane ( $hkl$ ),  $\lambda$  is the wavelength of the radiation, and  $d$  is the perpendicular distance between the reflecting planes with the indices  $h, k, l$ . X-ray radiation from a copper anode tube is monochromatized by thin nickel foils or curved crystal devices making Cu  $K_\alpha$  (1.5418 Å) the wavelength used most frequently. Any contribution from the continuous part of the copper spectrum, other copper spectral lines, incoherent scattering by the sample, or fluorescence is undesirable background. Theta is varied continuously and the  $d$ -spacings are derived by solution of the Bragg equation at the angles where diffraction maxima are observed.

A new X-ray diffraction technique utilizing polychromatic radiation and based on X-ray spectrography was introduced by Giessen and Gordon (1968). Crystals in the powder can coherently scatter (diffract) all wavelengths in the incident X-ray beam which correspond to their  $d$ -

spacing values. With the aid of a high resolution semiconductor detector, Giessen and Gordon performed a spectral analysis of the entire diffracted beam at a fixed angle  $\theta$ , and obtained a diffraction pattern from a platinum sheet. Compared to the conventional theta scanning X-ray powder techniques, the new method gathered information at a much greater rate. Recognizable patterns of platinum and rhenium metal sheets were produced in 15 seconds.

The relationship between the energy of a diffraction maximum ( $E$ ) and the interplanar spacing ( $d$ ) is best illustrated by rewriting the Bragg expression in terms of photon energy where:

$$E = hc/\lambda = 12.4/\lambda$$

and  $E$  is expressed in kiloelectron volts. The new form of the Bragg relationship is:

$$d(hkl) = (6.2/\sin \theta) \quad (1/E)$$

This paper applies the methodology developed by Giessen and Gordon (1968) in the collection of powder diffraction patterns of five common minerals. Quartz, calcite, kaolinite, chlorite, and muscovite powder diffraction patterns were obtained by the new method and compared to more standard ones. These minerals have a more complex crystal structure than the metals used previously and their diffraction patterns provide an excellent basis for evaluating the applicability of the new technique in determinative mineralogy. The new method is most appropriately described as energy dispersive X-ray powder diffractometry.

#### METHODOLOGY

An Ortec silicon detector was mounted in place of the standard detector on a General Electric XRD-5 diffractometer. The sample to detector distance was greater than normal because the assembly was placed temporarily on a mount outside the diffractometer arm. The diffraction angle was fixed at  $20^\circ 2\theta$  and lead shields were employed to exclude unwanted radiation. Samples were powdered and placed in the standard vertical sample holder. A potential of 35 KV at 15 ma was applied to the copper tube. Spectra were accumulated for 100 sec and typical count rates for the most intense diffracted beams were 5-10 counts per second. The rates of counting and data collection can be greatly increased by permanently mounting the detector closer to the sample. Diffractometer geometry is not critical.

A schematic illustration of the experimental apparatus affords a comparison with more standard conditions (Figure 1). The energy dispersive system employs a Si(Li) detector (surface area =  $30\text{mm}^2$ ) to collect the polychromatic diffracted beam. The diffraction angle is fixed by the diffractometer arm and collimating slits.

The multichannel analyzer used in these experiments had a 1024 channel memory. The detector was capable of operating over the energy range from 0 to 40 keV. In practice, this range extended from the detector threshold near 1 keV to the short wavelength cutoff at 35 keV. The Si(Li) detector assembly has an energy resolution of 207 eV for  $^{56}\text{Fe}$  at 5.898

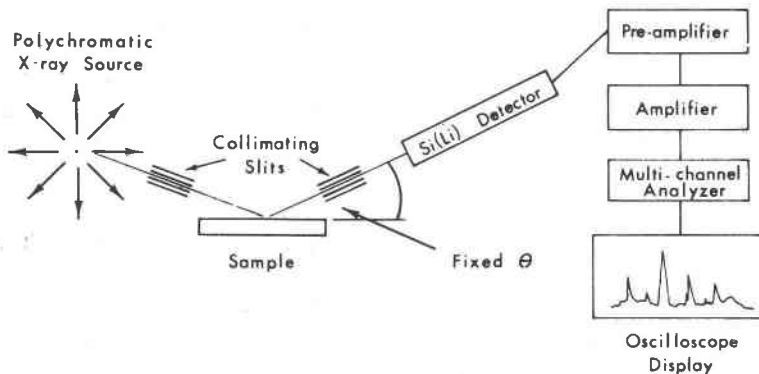


FIG. 1. Schematic diagram of energy dispersive x-ray powder diffractometer.

keV. Energy calibration of observed peaks was accomplished with a pulse generator. All system components were loaned by Ortec, Inc., of Oak Ridge, Tennessee.

#### QUARTZ DIFFRACTION PATTERN

A portion of the diffraction pattern obtained from a powdered sample of quartz illustrates the applicability of the energy dispersive technique to the identification of minerals (Figure 2). Nine diffraction maxima attributed to quartz peaks were recorded. The lower energy part of the spectrum contained reflected  $\text{Cu K}_\alpha$  and  $\text{Cu K}_\beta$  characteristic peaks, which obscured all diffraction peaks at lower energies. This interference can be reduced by changing the angle of diffraction and thereby shifting the position of the diffracted peaks.

In 100 seconds, it is possible to obtain a fairly good powder diffraction pattern for purposes of qualitative identification. The peaks are fairly well defined and easily observed above the background radiation. In as short a time as 10 seconds, the pattern can be recognized. The range in the  $d$ -spacings assigned to the midpoints of the peaks at half their maximum intensities was 3.34–1.41 Å. This is comparable to a  $40^\circ 2\theta$  scan from  $26^\circ$ – $66^\circ 2\theta$ .

The energy resolving capabilities of energy dispersive X-ray systems are poorer than the wavelength dispersive methods which employ crystals. The resolution of the silicon detectors does improve with increased energy, (Fitzgerald and Gantzer, 1970) but this is probably too small a change to appreciably reduce the peak widths. The improvement of detector resolution may ultimately reduce peak widths to 100 eV (Frankel and Aitken, 1970) but this probably would not improve significantly the observed pattern.

The width of the diffraction maximum at 10.7 keV is greater than 300 eV at half its maximum intensity. The base of this peak, attributed to

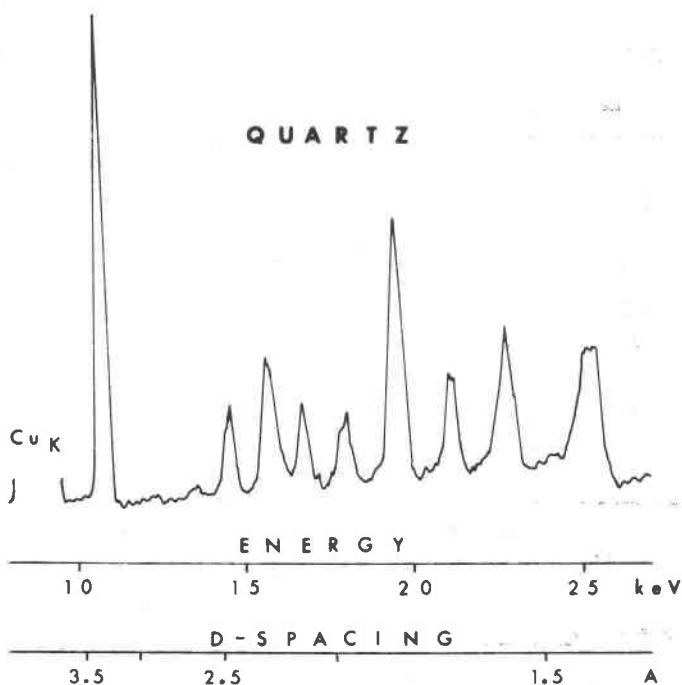


FIG. 2. X-ray powder diffraction pattern of quartz obtained with energy dispersive system. ( $\theta = 10^\circ$ ).

(101) diffraction from quartz, exceeds 600 eV. The  $d$ -spacing values covered by a peak this wide would range from 3.43 to 3.24 Å. The equivalent  $2\theta$  range in a  $\theta$ -scanning system would be from 26 to  $27.5^\circ 2\theta$ . The values are quite comparable, but the conventional  $\theta$ -scanning systems usually produce more sharply defined peaks. The differences in peak widths are probably the result of instrumental line-broadening effects and variations in crystallite sizes. Improving detector resolution will probably not benefit energy dispersive powder diffraction methods because the shorter  $d$ -spacing atomic planes increase the  $d$ -spacing resolving capability of  $\theta$ -scanning systems, at higher diffraction angles while the energy resolution of the Si(Li) detector remains essentially constant. The wide peaks produce considerable overlap between adjacent diffraction maxima and interfere with mineral identifications in polycomponent systems.

#### COMPARISON OF CALCULATED AND OBSERVED DIFFRACTION PATTERNS

Theoretical and observed diffraction data for quartz, calcite, kaolinite, chlorite, and muscovite are contained in Tables 1 through 5, respectively.

Table 1. X-ray Powder Diffraction Data of Quartz.

| $d^*(\text{A})^*$ | $I/I^*_{\text{max.}}$ | $(hkl)^*$ | $E(\text{keV})_{\text{calc.}}$ | $E(\text{keV})_{\text{obs}}$ | $d(\text{A})_{\text{obs}}$ | $I/I_{\text{max.}}$ |
|-------------------|-----------------------|-----------|--------------------------------|------------------------------|----------------------------|---------------------|
| 4.26              | 35                    | 100       | 8.3                            |                              |                            |                     |
| 3.34              | 100                   | 101       | 10.7                           | 10.7                         | 3.34                       | 100                 |
| 2.458             | 12                    | 110       | 14.5                           | 14.4                         | 2.48                       | 17                  |
| 2.282             | 12                    | 102       | 15.6                           | 15.7                         | 2.27                       | 28                  |
| 2.237             | 6                     | 111       | 16.0                           | 16.6                         | 2.15                       | 18                  |
| 2.128             | 9                     | 200       | 16.8                           | 17.8                         | 2.01                       | 16                  |
| 1.980             | 6                     | 201       | 18.0                           |                              |                            |                     |
| 1.817             | 17                    | 112       | 19.6                           | 19.3                         | 1.85                       | 53                  |
| 1.672             | 7                     | 202       | 21.4                           | 21.1                         | 1.69                       | 22                  |
| 1.695             | 3                     | 103       | 21.5                           | 22.7                         | 1.57                       | 30                  |
| 1.541             | 15                    | 211       | 23.2                           |                              |                            |                     |
| 1.453             | 3                     | 113       | 24.6                           | 25.2                         | 1.41                       | 24                  |

\*Data from ASTM card # 5-490

Table 2. X-ray Powder Diffraction Data of Calcite.

| $d^*(\text{A})^*$ | $I/I^*_{\text{max.}}$ | $(hkl)^*$ | $E(\text{keV})_{\text{calc.}}$ | $E(\text{keV})_{\text{obs}}$ | $d(\text{A})_{\text{obs}}$ | $I/I_{\text{max.}}$ |
|-------------------|-----------------------|-----------|--------------------------------|------------------------------|----------------------------|---------------------|
| 3.86              | 12                    | 102       | 9.25                           |                              |                            |                     |
| 3.035             | 100                   | 104       | 11.8                           | 11.8                         | 3.04                       | 100                 |
| 2.845             | 3                     | 006       | 12.5                           |                              |                            |                     |
| 2.495             | 14                    | 110       | 14.3                           | 14.2                         | 2.51                       | 16                  |
| 2.285             | 18                    | 113       | 15.6                           | 15.5                         | 2.30                       | 20                  |
| 2.095             | 18                    | 202       | 16.0                           | 16.9                         | 2.11                       | 21                  |
| 1.927             | 5                     | 204       | 18.5                           | 18.6                         | 1.92                       | 51                  |
| 1.913             | 17                    | 108       | 18.65                          |                              |                            |                     |
| 1.875             | 17                    | 116       | 19.0                           |                              |                            |                     |
| 1.626             | 4                     | 211       | 22.0                           | 21.8                         | 1.64                       | 16                  |
| 1.604             | 8                     | 212       | 22.25                          |                              |                            |                     |
| 1.587             | 2                     | 1,0,10    | 22.5                           | 23.1                         | 1.55                       | 17                  |
| 1.525             | 5                     | 214       | 23.4                           |                              |                            |                     |
| 1.518             | 4                     | 208       | 23.5                           |                              |                            |                     |
| 1.510             | 3                     | 119       | 23.65                          |                              |                            |                     |
| 1.473             | 2                     | 215       | 24.0                           | 24.5                         | 1.46                       | 13                  |

\*Data from ASTM card # 5-0586

Table 3. X-ray Powder Diffraction Data of Kaolinite.

| d*(A)* | I/I*<br>max. | (hkl)*            | E(keV)<br>calc. | E(keV)<br>obs | d(A)<br>obs | I/I<br>max |
|--------|--------------|-------------------|-----------------|---------------|-------------|------------|
| 7.18   | 100          | 001               | 5.0             | 5.0           | 7.14        | 17         |
| 4.48   | 80B          | 02-               | 8.0             | 10.1          | 3.53        | 67         |
| 3.58   | 100          | 002               | 10.0            | 10.3          | 3.47        | 28         |
| 2.565  | 80           | 20 $\bar{1}$ ,130 | 13.9            | 14.05         | 2.55        | 76         |
| 2.502  | 80           | 13 $\bar{1}$ ,200 | 14.3            |               |             |            |
| 2.386  | 80           | 003               | 15.0            | 15.2          | 2.35        | 100        |
| 2.341  | 90B          | 20 $\bar{2}$ ,131 | 15.25           | 15.9          | 2.25        | 52         |
| 2.206  | 10B          | 13 $\bar{2}$ ,201 | 16.2            | 17.7          | 2.02        | 63         |
| 1.989  | 40B          | 20 $\bar{3}$ ,132 | 18.0            |               |             |            |
| 1.789  | 40           | 004               | 19.0            | 21.0          | 1.70        | 76         |
| 1.666  | 50B          | 20 $\bar{4}$ ,133 | 21.45           |               |             |            |
| 1.541  | 10B          | 13 $\bar{4}$ ,203 | 23.15           | 23.4          | 1.53        | 52         |
| 1.488  | 100          | 060,33 $\bar{1}$  | 24.0            |               |             |            |

\*Data from ASTM card # 6-0221

Table 4. X-ray Powder Diffraction Data of Chlorite.

| d*(A)* | I/I*<br>max. | (hkl)*            | E(keV)<br>calc. | E(keV)<br>obs | d(A)<br>obs | I/I<br>max. |
|--------|--------------|-------------------|-----------------|---------------|-------------|-------------|
| 14.2   | 25           | 001               | 2.5             | 2.7           | 13.2        | 24          |
| 7.90   | 2            | --                | 4.57            |               |             |             |
| 7.14   | 100          | 002               | 5.0             | 4.9           | 7.28        | 47          |
| 4.774  | 90           | 003               | 7.5             |               |             |             |
| 4.595  | 2            | 020               | 7.75            |               |             |             |
| 3.964  | 2            | --                | 8.0             |               |             |             |
| 3.589  | 90           | 004               | 9.9             | 9.9           | 3.61        | 100         |
| 2.868  | 20           | 005               | 12.5            | 12.5          | 12.5        | 71          |
| 2.585  | 2            | 131,20 $\bar{2}$  | 13.8            | 13.5          | 2.64        | 71          |
| 2.442  | 2            | 132,20 $\bar{3}$  | 14.6            | 14.4          | 2.48        | 71          |
| 2.387  | 6            | 006,13 $\bar{3}$  | 15.0            | 15.4          | 2.30        | 53          |
| 2.048  | 6            | 007               | 17.4            | 17.3          | 2.06        | 88          |
| 2.015  | 2            | 204,135           | 17.7            |               |             |             |
| 1.893  | < 1          | 20 $\bar{6}$ ,135 | 18.8            | 18.4          | 1.94        | 59          |
| 1.793  | < 1          | 215               | 19.9            |               |             |             |
| 1.724  | 2            | 20 $\bar{7}$ ,136 | 20.7            | 20.9          | 1.71        | 47          |
| 1.674  | 4            | 206,13 $\bar{7}$  | 21.3            | 22.2          | 1.61        | 98          |
| 1.576  | 2            | 20 $\bar{8}$ ,137 | 22.8            |               |             |             |
| 1.538  | 2            | 060               | 23.2            |               |             |             |
| 1.503  | < 1          | 331,062           | 23.7            | 24.8          | 1.44        | 47          |

\*Data from ASTM card # 12-240

Table 5. X-ray Powder Diffraction Data of Muscovite.

| d*(A)* | I/I*<br>max. | (khl)*            | E(keV)<br>calc. | E(keV)<br>obs | d(A)<br>obs | I/I<br>max. |
|--------|--------------|-------------------|-----------------|---------------|-------------|-------------|
| 10.01  | >100         | 002               | 3.55            |               |             |             |
| 5.02   | 55           | 004               | 7.1             |               | 10.50       | 32          |
| 4.48   | 55           | 110               | 8.0             |               |             |             |
| 4.46   | 65           | 11 $\bar{1}$      | 8.0             |               |             |             |
| 4.39   | 14           | 021               | 8.1             |               |             |             |
| 4.30   | 21           | 111               | 8.3             |               |             |             |
| 4.11   | 14           | 022               | 8.65            |               |             |             |
| 3.973  | 12           | 112               | 9.0             |               |             |             |
| 3.889  | 37           | 11 $\bar{3}$      | 9.2             |               |             |             |
| 3.735  | 32           | 023               | 9.5             |               |             |             |
| 3.500  | 44           | 11 $\bar{4}$      | 10.2            |               |             |             |
| 3.351  | >100         | 006,024           | 10.6            | 10.6          | 3.37        | 60          |
| 3.208  | 47           | 114               | 11.2            |               |             |             |
| 2.999  | 47           | 025               | 11.9            |               |             |             |
| 2.871  | 35           | 115               | 12.4            | 12.1          | 2.96        | 40          |
| 2.803  | 22           | 11 $\bar{6}$      | 12.7            | 12.7          | 2.81        | 44          |
| 2.589  | 50           | 13 $\bar{1}$      | 13.8            | 13.8          | 2.57        | 100         |
| 2.580  | 45           | 116               | 13.85           |               |             |             |
| 2.562  | 90           | 202               | 14.0            |               |             |             |
| 2.514  | 20           | 008               | 14.2            |               |             |             |
| 2.458  | 19           | 13 $\bar{3}$      | 14.5            |               |             |             |
| 2.446  | 12           | 202               | 14.6            |               |             |             |
| 2.396  | 10           | 20 $\bar{4}$      | 14.9            | 14.8          | 2.41        | 52          |
| 2.380  | 24           | 133               | 15.0            |               |             |             |
| 2.247  | 12           | 22 $\bar{1}$ ,040 | 15.9            |               |             |             |
| 2.236  | 5            | 041               | 16.0            |               |             |             |
| 2.201  | 5            | 221               | 16.3            | 16.2          | 2.21        | 76          |
| 2.184  | 7            | 22 $\bar{3}$      | 16.4            |               |             |             |
| 2.149  | 10           | 222               | 16.7            | 16.6          | 2.15        | 72          |
| 2.132  | 23           | 043,135           | 16.8            |               |             |             |
| 2.051  | 6            | 044               | 17.4            |               |             |             |
| 2.010  | 75           | 00,10             | 17.7            | 17.7          | 2.02        | 32          |
| 1.975  | 14           | 137               | 18.1            |               |             |             |
| 1.736  | 6            | 139               | 20.6            |               |             |             |
| 1.699  | 6            | 150,24 $\bar{1}$  | 21.0            |               |             |             |
| 1.670  | 12           | 20,10             | 21.3            | 21.2          | 1.68        | 72          |
| 1.653  | 17           | 31 $\bar{4}$      | 21.6            |               |             |             |
| 1.602  | 7            | 313               | 22.2            |               |             |             |
| 1.499  | 40           | 33 $\bar{1}$ ,060 | 23.8            | 23.2          | 1.54        | 72          |

\*Data from ASTM card # 7-32

Theoretical energy values were calculated from the diffraction data on cards in the ASTM card file. The observed patterns always contained fewer peaks than anticipated. Lack of observed peak resolution and possible combinations are apparent in the tabulated data. The results are in

fairly good agreement with the expected  $d$ -values, but the intensities are highly variant.

The differences between the intensity values can be attributed to two major causes. Firstly, the intensities of X-rays generated at various wavelengths in the continuous spectrum are different. Secondly, the detector response varies with wavelength. The beryllium window of the detector absorbs more of the lower energy X-rays. In addition, air path absorption, differences in chemical composition, and the possibility of preferred orientation may also influence the observed intensities. The high intensities of diffraction maxima near 20 keV suggest that this region is where the above factors are optimally combined for enhancement. Intensities fall off toward the short wavelength cutoff and the characteristic copper lines.

#### ANALYSIS OF MULTIPLE COMPONENT MIXTURES

The analysis of a natural sedimentary rock sample containing quartz, calcite, kaolinite, and chlorite was attempted. The resultant pattern was difficult to interpret. The only diffraction peaks that could be identified with certainty were those of quartz. Quartz was about 50 percent by weight of the sample so the results are not surprising. There was only a slight indication of the presence of 8 percent calcite. Peak overlap was especially apparent.

The amount of peak overlap that might be observed in samples containing equal quantities of quartz and calcite is illustrated in Figure 3. The superimposed spectra have one peak each that would not be overlapped by a neighboring one. The (101) peak of quartz and the (104) calcite peak are separated. The Ca K characteristic peak would also help confirm the presence of calcite.

If the energy dispersive X-ray powder diffraction method is to be used in determining the mineralogy of multiple component systems, computing techniques should be employed. In principle, it is possible to formulate spectrum stripping routines with the use of high speed computers to analyze the diffraction patterns. The visual or manual interpretation of these spectra is difficult.

#### DISCUSSION

X-ray diffraction analyses with energy dispersive techniques have demonstrated applicability in the rapid identification of single mineral powders. In multiple component systems, however, the limited apparent resolution of the system is a handicap. Even with improvement of the operating efficiency of individual components the capabilities of the total system may not be enhanced significantly.

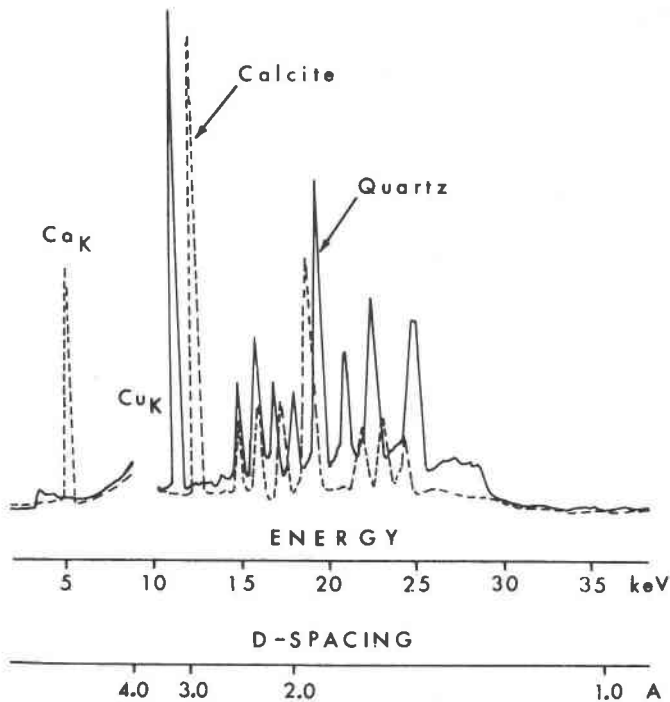


FIG. 3. Superimposed powder diffraction patterns of quartz and calcite illustrating the amount of peak overlap that would be present in a sample containing equal quantities of the two minerals.

The powder diffraction patterns may be observed with greater clarity by varying the instrument settings. A multichannel analyzer with more data storage channels might help to separate peaks. Adjusting  $\theta$  varies the range of  $d$ -spacing values observed and may improve the results. By changing  $\theta$  to  $45^\circ$  the range in  $d$ -spacings detected at the instrumental setting used above would be from 8.77 to 0.25 Å. In addition, the spectra may be simplified by altering the amplifier gain and thereby narrowing the range of diffracted energies observed at a given time. The use of an X-ray tube with a molybdenum or tungsten target could improve the results because the intensity of the "white" portion of the X-ray spectrum would be greater and the characteristic X-ray peaks would not be as prominent, or absent. These possibilities were not evaluated in the present study.

The detection of phase changes at elevated or depressed temperatures and pressures would appear to be one of the areas where this technique is most applicable. As Giessin and Gordon (1968) pointed out, reaction vessels need only contain one small X-ray exit port with this method.

Another important aspect of energy dispersive systems is worthy of note. The diffraction patterns contain peaks produced by secondary excitation of elements in the sample. Fluorescence analyses might be performed at the same time as diffraction analyses. Fitzgerald and Gantzer (1970) assessed an energy dispersive system as adequate for X-ray chemical analyses of characteristic spectra from 0.1 to 10 Å. The combined chemical and mineralogical determinations may offset the lack of diffraction peak resolution in some polymineralic analyses.

#### SUMMARY

Energy dispersive X-ray powder diffractometry of mineral samples can be readily accomplished in less than 100 seconds with a standard X-ray generator and goniometer. The use of a silicon semiconductor X-ray detector and a multichannel analyzer permits the simultaneous examination of a wide range of  $d$ -spacing values. Using a copper tube operated at 35 KV and 15 ma, and a fixed diffraction angle of  $20^\circ 2\theta$ , it is possible to measure interplanar atomic spacings from 35.69 to 1.02 Å.

The technique is readily applicable to the determination of unknown single mineral powders. In more complex mineral aggregates, the wide peak widths of the diffraction maxima produce serious overlap and complicate identification techniques. The method has limited use in applications that require accurate determinations of cell parameters. The rapidity of analysis and fixed geometry are the major advantages of energy dispersive systems. Simultaneous elemental analysis is an additional asset. Lack of resolving power is the major disadvantage.

#### ACKNOWLEDGMENTS

The author wishes to express his appreciation to Messrs. Gary Miller and Larry Albrecht of Ortec, Inc. for their assistance in arranging a demonstration of the energy dispersive system. Professor O. W. Albritton, Department of Engineering Mechanics, kindly permitted the use of a horizontal diffractometer. Drs. J. S. Hanor, S. A. Heath and C. H. Moore, read and offered suggestions to improve the manuscript. Without the photographic assistance provided by Messrs. P. B. Larimore and J. P. Kennedy the original diffraction data could not have been prepared for publication.

#### REFERENCES

- FITZGERALD, R., AND P. GANTZEL (1970) X-ray energy spectrometry in the 0.1–10 Å range. *Scripps Inst. Oceanography, Rep. SIO 70-20*.
- FRANKEL, R. S., AND D. W. AITKEN (1970) Energy dispersive X-ray emission spectroscopy. *Appl. Spectrosc.* **24**, 557–566.
- GIESSEN, B. C., AND G. E. GORDON (1968) X-ray diffraction: New high-speed technique based on X-ray spectrography. *Science* **159**, 973–975.

*Manuscript received, February 12, 1971; accepted for publication, May 20, 1971.*